

Supplemental Figures

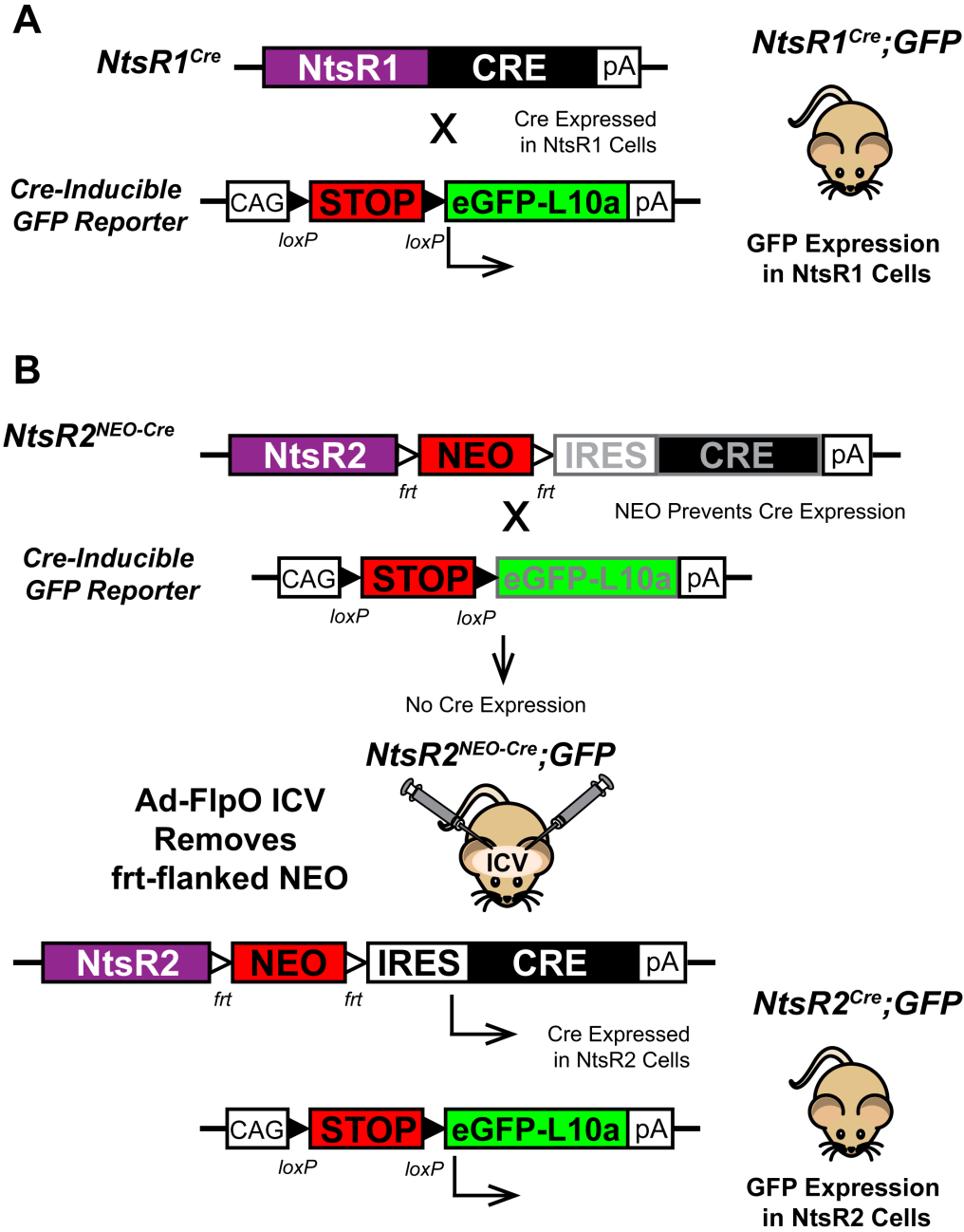


Figure S1. Generation of *NtsR1^{Cre};GFP* and *NtsR2^{Cre};GFP* reporter mice to visualize NtsR1 and NtsR2 neurons in the VTA, Related to Fig. 1. A) Commercially-available transgenic *NtsR1^{Cre}* mice were bred to a Cre-inducible GFP reporter line to generate mice expressing GFP selectively in NtsR1 neurons (*NtsR1^{Cre};GFP* mice). **B)** *NtsR2^{NEO-Cre}* mice were created by inserting an IRES-Cre sequence downstream of an *frt*-flanked NEO cassette directly into the NtsR2 locus using homologous recombination. *NtsR2^{NEO-Cre}* mice were then crossed to a Cre-inducible GFP reporter line, however GFP is not expressed because the NEO cassette prevents Cre expression. Thus, adult *NtsR2^{NEO-Cre};GFP* mice were injected with an adenovirus expressing Flp recombinase ICV to remove the *frt*-flanked NEO cassette, resulting in Cre and therefore GFP expression in NtsR2-positive cells (*NtsR2^{NEO-Cre};GFP* mice).

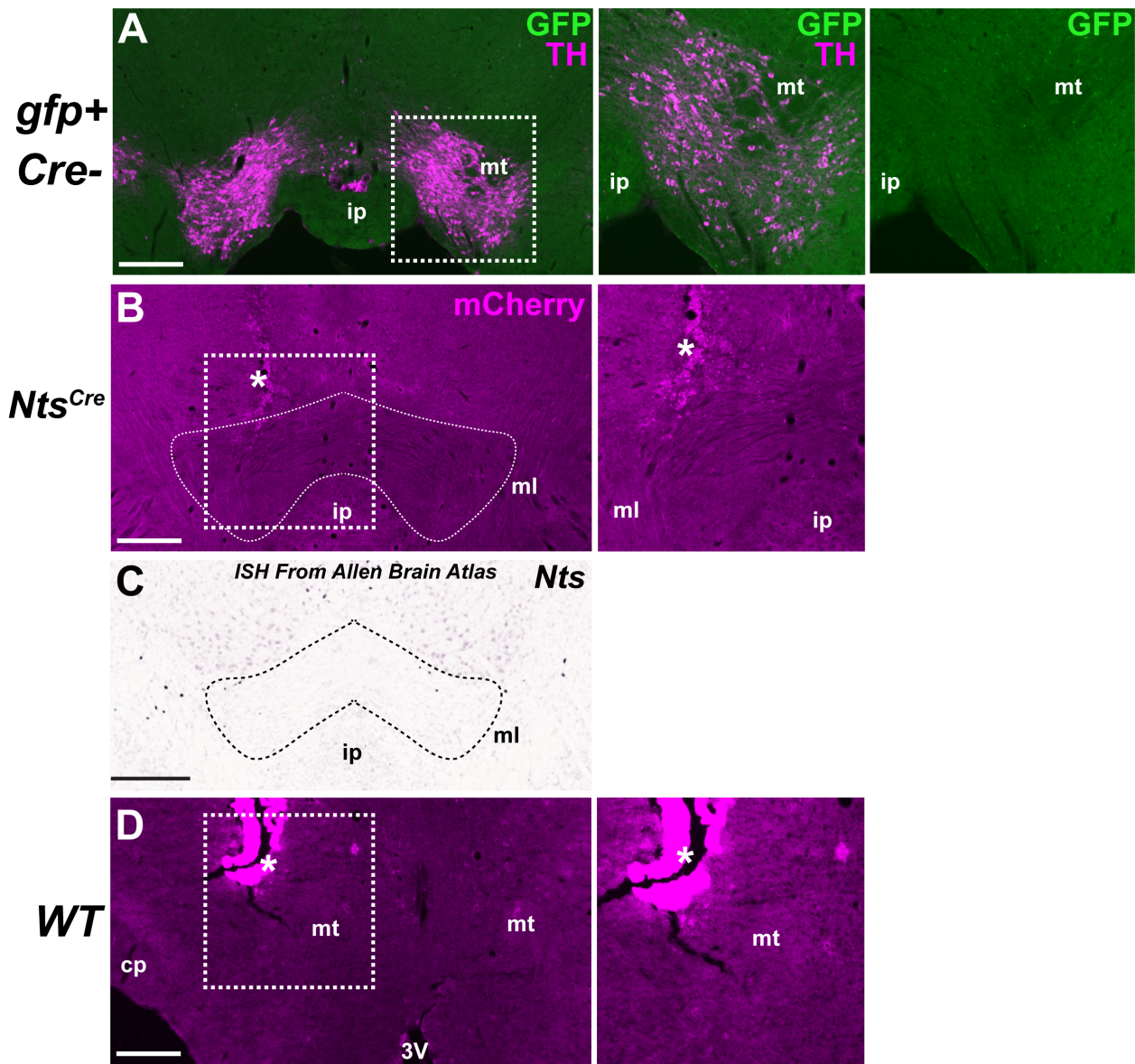


Figure S2. Validation of L10-eGFP reporter and Ad-syn-mCherry virus, Related to Figs. 1-2. **A)** Absence of L10-eGFP expression in mouse lacking cre, demonstrating that L10-eGFP is Cre-inducible. Panels represent magnified images of areas highlighted by dashed boxes. **B)** *Nts^{Cre}* mouse injected with Ad-syn-mCherry in the VTA, showing absence of mCherry-labeled cell bodies due to sparse *Nts* expression. **C)** *Nts* ISH in the VTA courtesy of the Allen Brain Atlas, confirming sparse *Nts* expression in the VTA (Lein et al., 2007). **D)** Wild-type (*WT*) mouse injected in the rostral lateral hypothalamic area showing no Ad-syn-mCherry expression. Injection tracts are indicated by (*). These data demonstrate that Ad-syn-mCherry requires Cre to be expressed. Scale bars represent 200 μ m in **A**, **B**, and **D** or 420 μ m in **C**. Abbreviations: ip=interpeduncular nucleus, ml=medial lemniscus, mt=mammillothalamic tract, cp=cerebral peduncle, 3V=third ventricle.

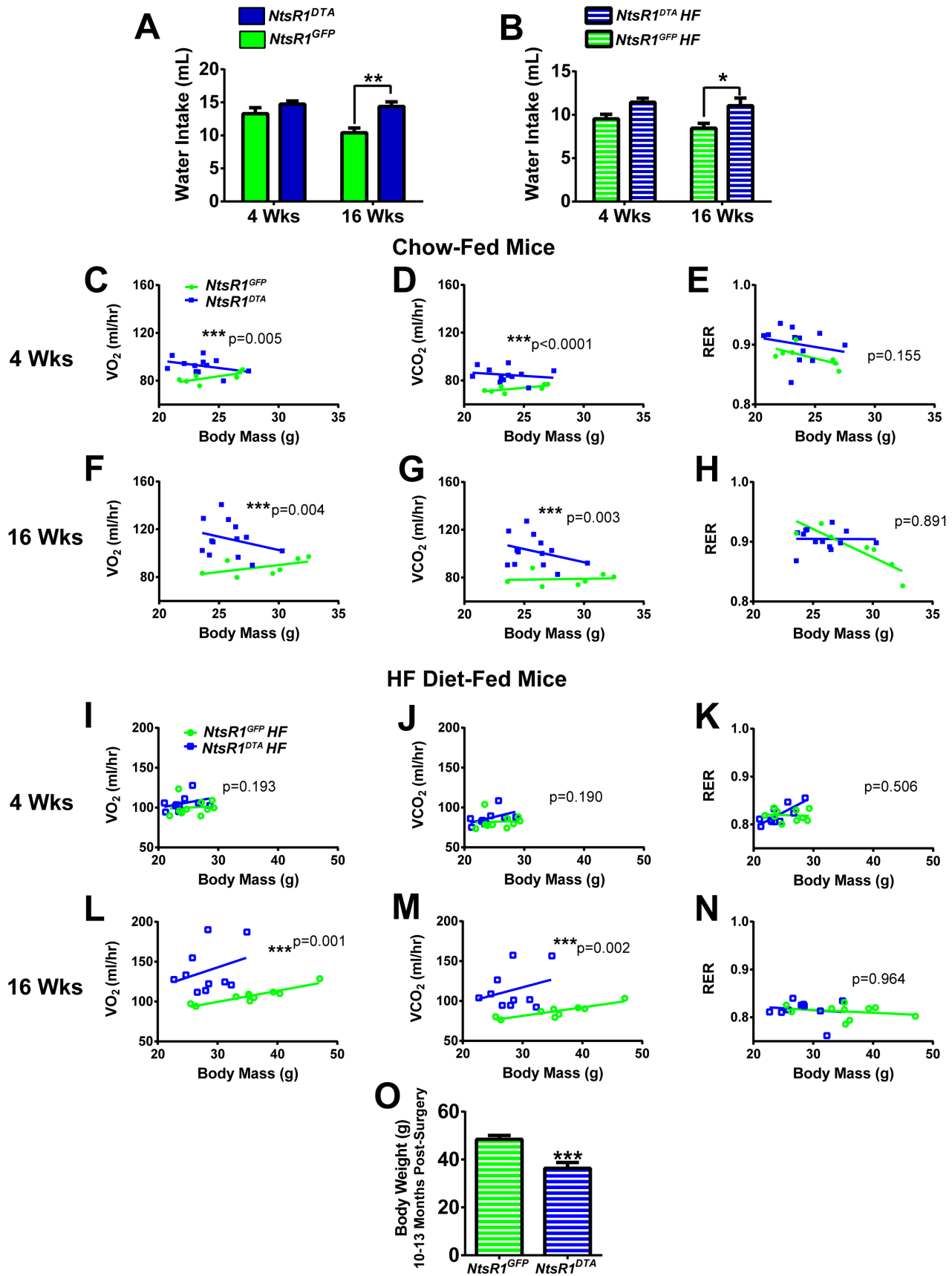
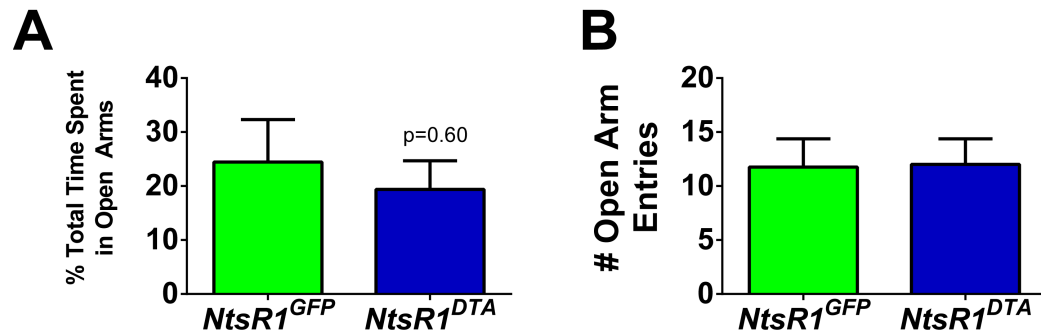


Figure S3. Fluid intake and metabolic assessment of *NtsR1^{GFP}* and *NtsR1^{DTA}* mice, Related to Fig. 3. Fluid intake and metabolic parameters were assessed over 4 days in TSE metabolic cages in *NtsR1^{GFP}* and *NtsR1^{DTA}* mice at 4 and 16 weeks post-surgery. Water consumption in **A)** chow-fed and **B)** HF diet-fed mice. Data represent mean \pm SEM, analyzed by two-way ANOVA. **C)** oxygen consumption (VO_2), **D)** carbon dioxide production (VCO_2) and **E)** respiratory exchange ratio (RER) at 4 weeks-post ablation in chow-fed animals. **F)** VO_2 , **G)** VCO_2 , and **H)** RER in chow-fed mice 16 weeks post-ablation. **I)** VO_2 , **J)** VCO_2 , and **K)** RER in HF diet-fed mice at 4 weeks. **L)** VO_2 , **M)** VCO_2 and **N)** RER in HF-diet fed mice 16 weeks post-ablation. All metabolic data were analyzed via ANCOVA to adjust for body weight as a covariate. **O)** Body weight of HF diet-fed mice at time of perfusion (10-13 months post-ablation), analyzed by unpaired t-test. (*NtsR1^{GFP}* n=7, *NtsR1^{DTA}* n=13, *NtsR1^{GFP}* HF n=10 and *NtsR1^{DTA}* HF n=10).



Figures S4. Anxiety-like behavior assessed via elevated-plus maze, Related to Fig. 5. No significant differences were found between groups in **A)** percentage of time spent on open arms or **B)** number of open arm entries (*NtsR1^{GFP}* n=4, *NtsR1^{DTA}* n=7).

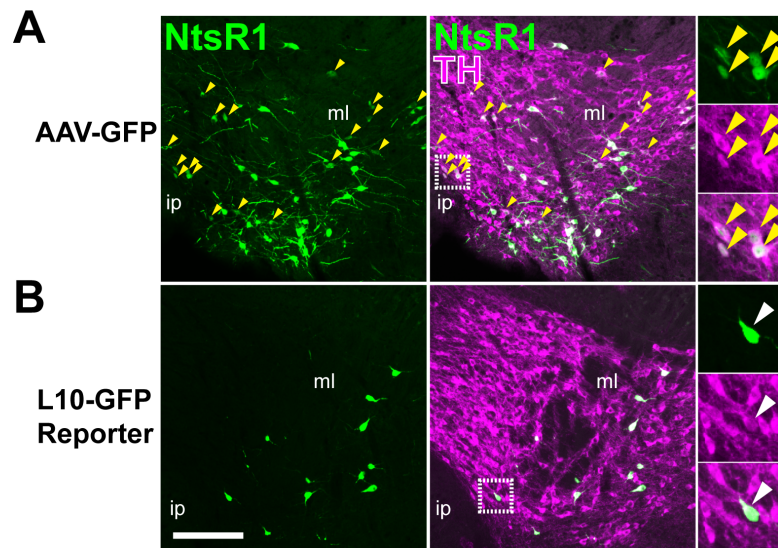


Figure S5. Virally-induced vs. endogenous GFP reporter expression for identification of VTA *NtsR1* neurons, Related to Figs. 1-3. **A)** GFP expression induced by Cre-inducible AAV-GFP injected into the VTA of *NtsR1^{Cre};GFP* transgenic mice. Yellow arrows indicate *NtsR1* neurons with reduced GFP expression that do not express endogenous L10-eGFP and colocalize with TH. **B)** Endogenous L10-eGFP expression in the VTA of uninjected *NtsR1^{Cre};GFP* mice reveals fewer labeled neurons compared to AAV-GFP-injected mice of the same genotype. Scale bar represents 100 μ m. Abbreviations: ip=interpeduncular nucleus, ml=medial lemniscus.

Supplemental Methods

Reagents

Recombinant leptin was purchased from the National Hormone and Peptide Program (Torrance, CA). The dopamine receptor-1 antagonist SCH233990 was purchased from Sigma (Saint Louis, MO). Amphetamine hydrochloride was from Cayman Pharmaceuticals (Ann Arbor, MI).

Generation of *NtsR2^{Cre}* Knock-In Mice

An *NtsR2^{Cre}* targeting vector was generated by inserting an IRES-Cre sequence between the stop codon and the polyadenylation site of the sequence encoding the 3' end of the mouse *NtsR2* gene, with an *frt*-flanked Neo cassette inserted upstream of the IRES-Cre. The linearized targeting vector was electroporated into mouse R1 embryonic stem (ES) cells (129sv background) and cells were selected with G418. DNA from ES cell clones was analyzed via qPCR for loss of homozygosity using Taqman primer and probes for the genomic *NtsR2* insertion site (F: ACCCATCAGATAAGCCATGC, R: GTGGGAAGTTGAGGGCAG, Probe: GTCTAAGCGGACCTACTGACCCA). *NGF* was used as a copy number control (Soliman et al., 2007). Putative positive ES clones were expanded, confirmed for homologous recombination by Southern blot and injected into mouse C57BL/6 blastocysts to generate chimeras. Chimeric males were mated with C57BL/6 females (Jackson Laboratory), and germline transmission was determined initially via progeny coat color and then confirmed via conventional PCR for IRES-Cre.

Genotyping

NtsR1^{Cre} and *NtsR2^{Cre}* mice were bred to C57BL/6J mice to maintain the lines, and progeny were genotyped via standard PCR (*NtsR1^{Cre}*: F: GACGGCAGCCCCCTTA, R: CGCAAACGGACAGAAGCATT, *NtsR2^{Cre}*: CCGTGTCTTCCTTCAGA, R: CTACACCTTGGTTGCACAGG).

Surgery

Mice received a pre-surgical injection of carprofen (5mg/kg *s.c.*) and were anesthetized with 3-4% isoflurane/O₂ in an induction chamber before being placed in a stereotaxic frame (Kopf). Under 1-2% isoflurane, access holes were drilled in the skull allowing a guide cannula with stylet (PlasticsOne) to be lowered into the brain target area. After 7 min to allow for AAV absorption, the injector and cannula were removed from the skull and the incision was closed using Vet Bond. *NtsR1^{GFP}* and *NtsR1^{DTA}* mice were monitored weekly for body weight after surgery, but did not undergo analysis until 4 wks post-surgery to allow DTA-mediated cell death to occur. Due to the limited production of *NtsR1^{Cre}* mice in our breeding colony, we generated 6 staggered cohorts of mice, each containing mice injected with AAV-GFP or AAV-DTA. We injected approximately twice as many mice with AAV-DTA as AAV-GFP, reasoning that after exclusion of mis-targeted AAV-DTA mice (with insufficient ablation), we would have roughly equally sized groups of 6-8 mice. Although cohorts were independently studied, they were perfused at the same time for simultaneous post-hoc assessment of bilateral VTA targeting. Mice were only included in the final study if injections were localized to and contained within the VTA. For *NtsR1^{DTA}* mice, this was determined by specific lack of GFP expression in the VTA. After post-hoc examination, 2/15 *NtsR1^{DTA}* and 3/13 *NtsR1^{DTA-HF}* mice were excluded due to unilateral targeting and/or spread of the injection site to the substantia nigra (SN), leaving *NtsR1^{GFP}* = 7 and *NtsR1^{DTA}* = 13; *NtsR1^{GFP}* HF=10 and *NtsR1^{DTA}* HF=10 for final analysis. To visualize NtsR2 neurons, adult male and female *NtsR2^{Cre}*; *GFP* were bilaterally injected with 1 μ L FLP adenovirus (Vector Biolabs) into the lateral ventricles in accordance with the atlas of Paxinos and Franklin (Keith B.J. Franklin, 2007): A/P: -0.22, M/L: +/- 1.0, D/V: -2.0. Mice were perfused 10 days after surgery to permit sufficient time for FLP-mediated excision of the *frt*-flanked Neo cassette and GFP expression. For tracing studies, *NtsR1^{Cre}* mice were injected unilaterally in the VTA with 75-100nL of an anterograde Cre-inducible adenovirus expressing a synaptophysin-mCherry fusion protein, Ad-syn-mCherry (Opland et al., 2013) using the same coordinates described in main text. Mice recovered for 7-10 days after surgery to allow for synaptophysin-mCherry expression at pre-synaptic terminals.

Sucrose Preference

NtsR1^{DTA} and *NtsR1^{GFP}* mice were given two identical 50 mL sipper bottles in their home cages for 4 consecutive days. On days 1-2, both bottles were filled with water to acclimate the animals to the test environment. On days 3-4, one bottle was switched to 0.5% sucrose while the other contained water. The bottle positions were rotated daily to avoid position bias, and the volume consumed from each bottle was measured at the same time each day. To assess leptin-induced changes in sucrose preference, animals were re-tested one month later for 6 consecutive days.

On days 1-2, animals received once daily sham intraperitoneal (*ip*) injections while both bottles contained water. On day 3, one bottle was switched to 0.5% sucrose. Mice were treated with PBS on days 3-4 and leptin (5mg/kg *ip*) on days 5-6. All injections were administered at the onset of the dark cycle when most food and water intake naturally occurs. Data are reported as sucrose preference, which is the percentage of sucrose consumed out of total liquid consumed.

Operant Testing (Expanded)

Based on previous work (Sharma et al., 2012), mice were food restricted to 90% of their body weight and trained on a fixed ratio-1 (FR1) schedule until they achieved 75% response accuracy with ≥ 20 rewards earned on 3 consecutive days. Training sessions were terminated after 1 hr or when the animal had earned 50 rewards. Mice achieving these criteria were then switched to *ad lib* food and trained on an FR5 schedule for 3 consecutive days. On test days, mice were subject to a progressive ratio (PR) schedule where $PR = [5e^{(R*0.2)}] - 5$ with R=number food rewards earned+1 (Richardson and Roberts, 1996). Thus, the number of correct responses needed to earn a sucrose reward increases as follows: 1, 2, 4, 6, 9, 12, 15, 20, 25, 32, 40, 50, 62, 77, 95 *etc.* The PR breakpoint was recorded as the highest ratio completed for each 1 hr test session. Mice were tested until they achieved stable PR which was defined as <10% variation in rewards earned over 3 consecutive sessions.

Elevated Plus Maze

Mice were assessed for anxiety-like behavior using an elevated plus maze (EPM) as previously described (Eagle et al., 2015). Briefly, the EPM apparatus was custom-built based on plans from ANY-maze (www.anymaze.com, Stoelting Co.) and mice were given free access to the open and closed arms for 5 minutes. Their behavior was recorded using a digital CCD camera and the percentages of time spent in the open and closed arms were analyzed using Topscan automated video tracking software (Clever Sys).

Immunohistochemistry and Immunofluorescence

Mice were treated with a lethal dose of *ip* pentobarbital followed by transcardial perfusion with 10% neutral-buffered formalin (Fisher Scientific). Brains were removed, post-fixed in 10% formalin overnight at 4°C, dehydrated with 30% sucrose in PBS for 2-3 days, and sectioned into 30 μ m slices using a sliding microtome (Leica). Brain sections were then analyzed by immunofluorescence or immunohistochemistry as previously described (Leininger et al., 2011; Opland et al., 2013). For characterization of NtsR1 and NtsR2 expression, sections from *NtsR1^{Cre};GFP* and *NtsR2^{Cre};GFP* mice were stained with chicken anti-GFP (1:2000, Abcam), mouse anti-TH (1:1000, Millipore), or rabbit anti-S100 (1:1000, Abcam), followed by incubation with species-specific secondary antibodies conjugated to AlexaFluor 488 or 568 fluorophores (Life Technologies or Jackson ImmunoResearch). For ablation studies, *NtsR1^{DTA}* and *NtsR1^{GFP}* mice were treated with PBS or amphetamine (4mg/kg) (Yates et al., 2007) 90 minutes prior to perfusion, and brain sections were stained for cFos (1:500, goat, Santa Cruz) with secondary detection via DAB (Life Technologies), followed by immunofluorescent detection of GFP, TH, or DAT (1:1000, Millipore) as described above. Most tissues were analyzed using an Olympus BX53 fluorescence microscope outfitted with transmitted light to analyze DAB-labeling, as well as FITC and Texas Red filters. Images were collected using Cell Sens software and a Qi-Click 12 Bit cooled camera. Sections stained for GFP and S100 or TH were also analyzed using a Nikon C2 confocal laser scanning microscope under a Plan Fluor 10x DIC L N1 objective with FITC (excitation 488nm) and Texas Red (excitation 561 nm) filters. Images were analyzed using Photoshop software (Adobe) and in some cases, brightness and/or contrast adjustments were uniformly applied to images. For quantification and colocalization of NtsR1 and NtsR2 neurons with TH, five representative sections spanning the entire VTA were selected from each mouse, from which all GFP and/or TH positive neurons were counted. For Ad-syn-mCherry tracing experiments, terminal density was qualitatively assessed by 1) comparing side-by-side images of each brain area from multiple animals and 2) generating a map of innervation patterns for each animal based on the Paxinos brain atlas.

Gene Expression

At 16 weeks post-surgery, *NtsR1^{DTA-Uni}* (n=17) and *NtsR1^{GFP-Uni}* (n=7) were deeply anesthetized with sodium pentobarbital and tissue from the injected and uninjected sides of the VTA and NA were separately microdissected. Tissue was immediately snap frozen on dry ice and stored at -80°C for later processing. RNA was extracted using Trizol (Invitrogen, Carlsbad, CA) and 200 ng samples were converted to cDNA using the Superscript First Strand Synthesis System for RT-PCR (Invitrogen, Carlsbad, CA). Sample cDNAs were analyzed in triplicate via quantitative RT-PCR for gene expression using TaqMan reagents and an ABI 7900 (Applied Biosystems) at the

MSU Genomics Core. With *GAPDH* expression as an internal control, relative mRNA expression values were calculated by the $2^{-\Delta\Delta Ct}$ method and normalized to the uninjected side of each mouse. To verify targeting, *Ntsr1*^{DTA-Uni} mice were considered sufficiently ablated if the fold change in *Ntsr1* expression was less than 1 standard deviation below the mean *Ntsr1* fold change in AAV-GFP-injected mice. By this criterion, 7 of 15 *Ntsr1*^{DTA-Uni} mice were deemed insufficiently ablated and were excluded from the analysis.

Supplemental References

Eagle, A.L., Gajewski, P.A., Yang, M., Kechner, M.E., Al Masraf, B.S., Kennedy, P.J., Wang, H., Mazei-Robison, M.S., and Robison, A.J. (2015). Experience-Dependent Induction of Hippocampal DeltaFosB Controls Learning. *The Journal of neuroscience : the official journal of the Society for Neuroscience* 35, 13773-13783.

Keith B.J. Franklin, G.P. (2007). *The Mouse Brain In Stereotaxic Coordinates*. (Elsevier).

Lein, E.S., Hawrylycz, M.J., Ao, N., Ayres, M., Bensinger, A., Bernard, A., Boe, A.F., Boguski, M.S., Brockway, K.S., Byrnes, E.J., et al. (2007). Genome-wide atlas of gene expression in the adult mouse brain. *Nature* 445, 168-176.

Leinninger, G.M., Opland, D.M., Jo, Y.H., Faouzi, M., Christensen, L., Cappellucci, L.A., Rhodes, C.J., Gnegy, M.E., Becker, J.B., Pothos, E.N., et al. (2011). Leptin action via neurotensin neurons controls orexin, the mesolimbic dopamine system and energy balance. *Cell metabolism* 14, 313-323.

Opland, D., Sutton, A., Woodworth, H., Brown, J., Bugescu, R., Garcia, A., Christensen, L., Rhodes, C., Myers, M., Jr., and Leinninger, G. (2013). Loss of neurotensin receptor-1 disrupts the control of the mesolimbic dopamine system by leptin and promotes hedonic feeding and obesity. *Molecular metabolism* 2, 423-434.

Richardson, N.R., and Roberts, D.C. (1996). Progressive ratio schedules in drug self-administration studies in rats: a method to evaluate reinforcing efficacy. *Journal of neuroscience methods* 66, 1-11.

Sharma, S., Hryhorczuk, C., and Fulton, S. (2012). Progressive-ratio responding for palatable high-fat and high-sugar food in mice. *Journal of visualized experiments : JoVE*, e3754.

Soliman, G.A., Ishida-Takahashi, R., Gong, Y., Jones, J.C., Leshan, R.L., Saunders, T.L., Fingar, D.C., and Myers, M.G., Jr. (2007). A simple qPCR-based method to detect correct insertion of homologous targeting vectors in murine ES cells. *Transgenic research* 16, 665-670.

Yates, J.W., Meij, J.T., Sullivan, J.R., Richtand, N.M., and Yu, L. (2007). Bimodal effect of amphetamine on motor behaviors in C57BL/6 mice. *Neuroscience letters* 427, 66-70.